Response to reviewers

Preprint wes-2025-41

Title: Scour variability across offshore wind farms (OWFs): Understanding site-specific scour drivers as a step towards assessing potential impacts on the marine environment

Authors: Karen Garcia, Christian Jordan, Gregor Melling, Alexander Schendel, Mario Welzel, Torsten Schlurmann

Authors' reply to comments

We sincerely thank the reviewer for taking the time to evaluate our work and for recognizing its contributions. After carefully reading and discussing the remarks, we have thoroughly revised and improved the manuscript accordingly. Please find our responses (blue) and revised text blocks (*blue*, *italic*) below the quoted reviewer comments (black). Please note that, in the meantime, we have revised the data, added new equations and generated new figures to improve the manuscript based on the reviewer's comments. Moreover, we included a few minor changes that might not refer directly to specific reviewer comments but are meant to enhance the readability and hence understanding of our approach and findings according to a native speaker.

**Response to Referee # 1**

1. The paper investigates the variability of scour depths around monopile foundations in offshore wind farms (OWFs) and identifies the key drivers influencing these scour processes. The study utilizes high-resolution bathymetry data from 460 monopiles across nine British OWFs to analyze spatial and environmental factors affecting scour. It should be acknowledged that the measurement data from the present study are of great engineering value to predict the scour before the planning of OWF. The methodology of interpreting the data is reasonable, and the general conclusion from the interpretation is plausible. The primary problem is that the overall manuscript lacks physical analysis and correlation of the scour depth with the hydrodynamic quantities. This is understandable due to the lack of critical Shield parameters, which are directly linked to the scour process. Furthermore, in shallow water regions, it seems that the wave characteristics associated with the KC number play an important role in determining the scour depth. As pointed out by the authors, this parameter is not analyzed due to the limited measurement. Despite this lack, the physical interpretation of this manuscript can still be enhanced by estimating the values of the Shields and KC based on some assumptions. For example, combined with Re and the roughness associated with the grain size, the shear stress can be estimated based on a log law assumption. Combined with the dispersion relationship, knowing the water depth, the wave-induced velocity can be estimated so that the KC value can be estimated.

Dear Referee #1,

1. The authors appreciate the reviewer's most valuable comment and appreciate the recognition of the value of our study in analyzing the variability of scour depths around monopile foundations at offshore wind farms (OWFs). We are pleased that the reviewer acknowledges the engineering value of the high-resolution bathymetry data of 460 monopiles at nine UK OWFs and the methodology used to interpret these data.

We fully concur with the critical observation regarding the need for a more in-depth physical analysis, specifically the correlation of scour depths with key hydrodynamic parameters such as the Shields parameter *($\theta_{99}$)* and the Keulegan-Carpenter number *($KC_{99}$)*. The reviewer correctly identified these parameters as fundamental to the scour process. We acknowledge that their absence from the initially submitted manuscript limits the ability to interpret the findings systematically.

In response, equations 9 and 19 were used and are included in Table 2 on pages 10-11 to calculate the $KC_{99}$ and $\theta_{99}$, respectively:

***Table 2.*** *Calculation of the variables included in the analysis*

| *Variable* | *Equation* | |
|---|---|---|
| *Zero crossing period* ($\boldsymbol{T_z}$) | $T_z = \frac{T_p}{1.28}$ | *(8a)* |
| *Natural scaling period* ($\boldsymbol{T_n}$) | $T_n = \sqrt{\frac{h}{g}}$ | *(8b)* |
| ($\boldsymbol{A_t}$) | $A_t = (6500 + \left(0.56 + 15.54\frac{T_n}{T_z}\right)^6)^{1/6}$ | *(8c)* |
| *RMS velocity* ($\boldsymbol{U_{rms}}$) | $U_{rms} = 0.25\frac{H}{T_n(1 + \left(A_t\left(\frac{T_n}{T_z}\right)^2\right))^3}$ | *(8d)* |
| *Wave-induced velocity* ($\boldsymbol{U_m}$) | $U_m = \sqrt{2}\,U_{rms}$ | *(8e)* |
| *Keulegan-Carpenter number* ($\boldsymbol{KC}$) | $KC_{99} = \frac{U_m T_p}{D}$ | *(9)* |
| *Roughness related to* $\boldsymbol{d_{50}}$ ($\boldsymbol{ks}$) | $k_s = 2.5d_{50}$ | *(10)* |
| *Amplitude of wave orbital motion at the bed* ($\boldsymbol{A}$) | $A = \frac{U_m T_p}{2\pi}$ | *(11)* |
| *shear velocity* ($\boldsymbol{U_f}$) | $U_f = \frac{U}{6.0 + 2.5\ ln\left(\frac{h}{k_s}\right)}$ | *(12)* |
| *wave friction factor* ($\boldsymbol{f_w}$) | $f_w = \begin{cases} 0.32\left(\frac{A}{k_s}\right)^{-0.8}, & \frac{A}{k_s} < 2.92 \\ 0.237\left(\frac{A}{k_s}\right)^{-0.52}, & 2.92 \le \frac{A}{k_s} < 727 \\ 0.04\left(\frac{A}{k_s}\right)^{-0.25}, & \frac{A}{k_s} \ge 727 \end{cases}$ | *(13)* |
| *angular difference between the direction of* | $\alpha = atan2(u_0, v_0) - D_w$ | *(14)* |

| | | |
|---|---|---|
| *the wave and the current* ($\boldsymbol{\alpha}$) | | |
| *current induced bed shear stress* ($\boldsymbol{\tau_c}$) | $\tau_c = \rho_w U_f^2$ | *(15)* |
| *wave induced bed shear stress* ($\boldsymbol{\tau_w}$) | $\tau_w = 0.5\rho_w f_w U_m^2$ | *(16)* |
| *cycle-mean shear stress* ($\boldsymbol{\tau_m}$) *due to a combined wave-current load* | $\tau_m = \tau_c \left[1 + 1.2\left(\frac{\tau_w}{\tau_c+\tau_w}\right)^{3.2}\right]$ | *(17)* |
| *maximum shear stress value under combined wave-current load* ($\boldsymbol{\tau_{max}}$) | $\tau_{max} = [(\tau_m + \tau_w \cos\alpha)^2 + (\tau_w \sin\alpha)^2\ ]^{0.5}$ | *(18)* |
| *Shields parameter* ($\boldsymbol{\theta}$) | $\theta_{99} = \dfrac{\tau_{max}}{(\rho_s - \rho_w) g d_{50}}$ | *(19)* |
| *Mobility parameter* $\boldsymbol{\theta_{99}}/\boldsymbol{\theta_{cr}}$ | $\theta_{99}/\theta_{cr}$ | *(20)* |

Lines 220-235 which follow Table 2, have been modified to describe the assumptions, physical meaning and relevance of these new parameters:

*The values assumed for all OWFs sites are:*

$$\rho_s = 2650\ kg/m^3, \rho_w = 1027\ kg/m^3, v = 1.3x10^{-6} m^2/s, g = 9.8\ m/s^2$$

*Where $\rho_s$ is the sediment density, based on Soulsby (1997). $\rho_w$ is the water density, $v$ is the kinematic viscosity and g the gravitational acceleration. Equation 4 was calculated based on van Rijn (1984), where $D_*$ is the non-dimensional grain diameter that is used to calculate the critical Shields parameter ($\theta_{cr}$), which represents the threshold for initiation of motion at the bed, as proposed by Soulsby (1997).*

*Equation 5 is taken from Soulsby and Whitehouse (1997), where s ($s = \rho_s/\rho_w$) represents the specific gravity of sediment grains. The $d_{50}$ represents the median sediment grain size.*

*In equation 18, the maximum bed shear stress value ($\tau_{max}$) was calculated following Roulund et al. (2016), which builds upon Soulsby (1997) by combining current- and wave-induced shear stress through a directional correction. Shields parameter ($\theta_{99}$) is derived using equation 19, based on the maximum bed shear stress ($\tau_{max}$) under combined wave and current conditions. The Keulegan–Carpenter number ($KC_{99}$) is defined in equation 10, where $T_p$ is the peak wave period and D the monopile diameter.*

*Equation 20 provides the calculation of the mobility parameter ($\theta_{99}/\theta_{cr}$) to assess sediment mobility, providing a dimensionless indicator of whether the hydrodynamic forcing was sufficient to initiate sediment motion. All relevant equations are summarized in table 2.*

Due to the consideration of parameters such as Keulegan-Capenter number, and sediment mobility $(\theta_{99}/\theta_{cr})$ parameter, together with the concern of reviewer 2, in regards of the choice of a mix of dimensionless and dimensional parameters in the PCA, The figure 4, which represents the PCAhas been updated with the considerations of just dimensionless parameters (Figure 5 and 6 have been also updated, and added in the manuscript), see in page 18:

***a)***

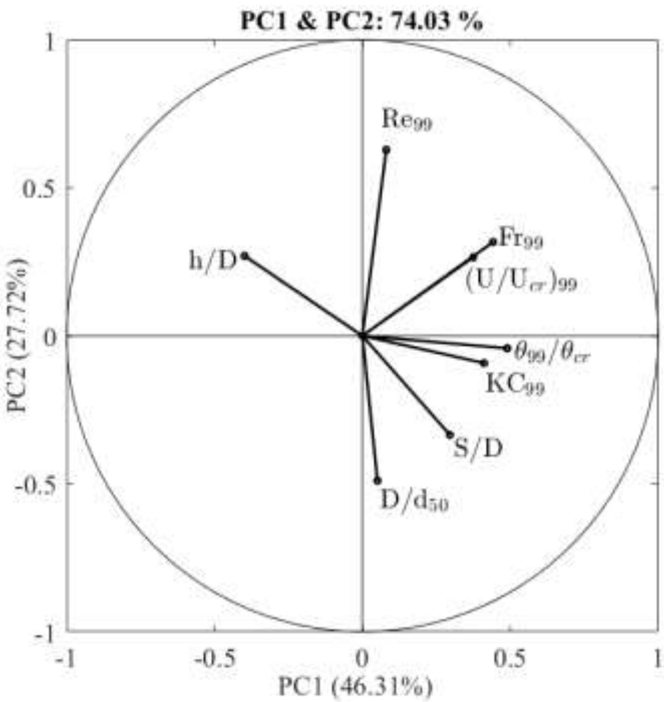


***b)***

| *Variables* | *θ to S/D* | *Cosine-based Correlation with S/D* |
|---|---|---|
| $\boldsymbol{h/D}$ | ***165.59*** | ***0.96*** |
| $\boldsymbol{D/d_{50}}$ | ***35.52*** | ***0.81*** |
| $\boldsymbol{KC_{99}}$ | ***35.91*** | ***0.81*** |
| $\boldsymbol{\theta_{99}/\theta_{cr}}$ | ***43.60*** | ***0.72*** |
| $Re_{99}$ | *131.21* | *0.65* |
| $(U/U_{cr})_{99}$ | *83.84* | *0.11* |
| $Fr_{99}$ | *84.17* | *0.10* |

***Figure 4: a) PCA biplot, illustrating the correlation between dimensionless variables and relative scour depths. b) The table details the angles between $S/D$ and the other variables (in degrees), along with the magnitude cosine-based correlation (values from 0 to 1), where values closer to 1 indicate stronger correlation.***

Lines 3368-410 (Page 18 -19), which describe the results from the PCA, have been modified:

*"As shown in the biplot, PC1 and PC2 account for 74.03% of the variation in the data set. This high percentage indicates that these two components capture most of the significant patterns in the data, allowing for a meaningful interpretation of the relationships among the variables. In the biplot, each vector stands for a variable, with the direction and magnitude of the vector reflecting its contribution to the principal components. The variables that contribute the most to the variance in PC1 are the mobility parameter , the Froude number, and Keulegan Carpenter number, with shares of 0.4898, 0.4419, and 0.4114, respectively. In contrast, the variance in PC2 is primarily explained by the pile Reynolds number (, the relative grain size and the Froude number, with shares of 0.628, -0.489, and 0.3168, respectively. This significant contribution of the mobility parameter, the Froude number, and the Keulegan Carpenter number to PC1*

*suggests that variations in these hydrodynamic parameters are critical in shaping the principal dynamics of the dataset.*

*The table (Fig. 4b) next to the biplot provides further insight by showing the angular distances between the $S/D$ vector and each of the other variables, as well as their respective correlation coefficients. One of the key observations is that the relative scour depth has the strongest negative correlation of 0.96 with the relative water depth, which underscores the critical role of water depth in governing scour intensity. Shallower relative depths concentrate flow energy at the bed, intensifying near-bed velocities and shear stresses that promote deeper scour holes (Smith & McLean, 1977; Whitehouse, 2010). The next strongest correlation is with the relative grain size with a correlation factor of 0.81. This suggests that as the relative grain size increases, relative scour depth also tends to increase. This trend is in line with the functional dependence of relative scour depth on relative grain size as observed by Sheppard et al. (1995, 1999). This positive trend may be due to increased turbulence caused by larger bed roughness elements or the initiation of larger-scale scour processes around coarser particles under certain flow conditions (Whitehouse, 2010).*

*Furthermore, a significant positive correlation was found with the Keulegan-Carpenter number with a correlation factor of 0.81, indicating the importance of oscillatory flow conditions in scour development. Higher Keulegan Carpenter numbers directly lead to higher relative scour depths (Sumer and Fredsoe, 2002). This is driven by the onset of the horseshoe vortex and lee-wake eddy shedding (Sumer et al., 1992b; Zanke et al., 2011), with increased permanence of the horseshoe vortex and amplification of bed shear stresses at higher KC values (Sumer et al., 1997). In addition, the mobility parameter exhibits a strong positive correlation (0.71) with the relative scour depth. The mobility parameter quantifies the instantaneous capacity of the flow to exceed the entrainment threshold, driving rapid sediment entrainment when significantly above unity (Soulsby, 1997; van Rijn, 1993). Variables such as the pile Reynolds number, the flow intensity , and the Froude number, although less correlated with relative scour depths, contribute more to the total variance. This suggests that these flow-related variables influence relative scour depths through more complex or non-linear interactions with other hydrodynamic conditions and sediment characteristics.*

*Since seabed sediment characteristics play a significant role in local scour (Qi et al., 2016), the PCA was applied again to the same dataset but pre-clustered into different soil classes (Annad et al. 2021). By reducing the uncertainties related to the grain size ($d_{50}$), this analysis should provide a better estimation of the local scour. This classification also facilitates the identification of parameters that are more influential in estimating scour for specific soil classes rather than uniformly across different types. After the clustering, six soil classes were obtained: cohesive sediment ($d_{50}$ ≤63 $\mu m$) with 5 data points, fine sand ($63 \leq d_{50} < 200\ \mu m$) with 203 data points, medium sand ($200 \leq d_{50} < 630\ \mu m$) with 249 data points, coarse sand ($630$*

*$\leq d_{50} <$ 2000 $\mu m$) with 170 data points, fine gravel (2000 $\leq d_{50} <$ 6300 $\mu m$) with 18 data points, and medium gravel ($d_{50} \geq$ 6300 $\mu m$) with 49 data points.*

After the results of the new PCA (Figure 4), where relative scour depth is correlated with four parameters such as the relative water depth ($S/D$), the relative grain size ($^{D}/_{d_{50}}$), the Keulegan-Carpenter number ($KC_{99}$) and the mobility parameter ($^{\theta_{99}}/_{\theta_{cr}}$), a new figure was also added into the manuscript (fig.9) which shows the new correlations between relative scour depth with the Keulegan Carpenter number (fig. 9a) and the mobility parameter (fig. 9b), In addition, figure 7 now represents the correlation of relative scour depth with relative water depth (which was presented in the first version of the manuscript as a figure 8), followed by Figure 8, showing the correlation between relative scour depth and relative grain size (Figure 8a), and the correlation between relative scour depth and grain size (Figure 8b).Those figures were added in pages 29 and  32-, L626-694:

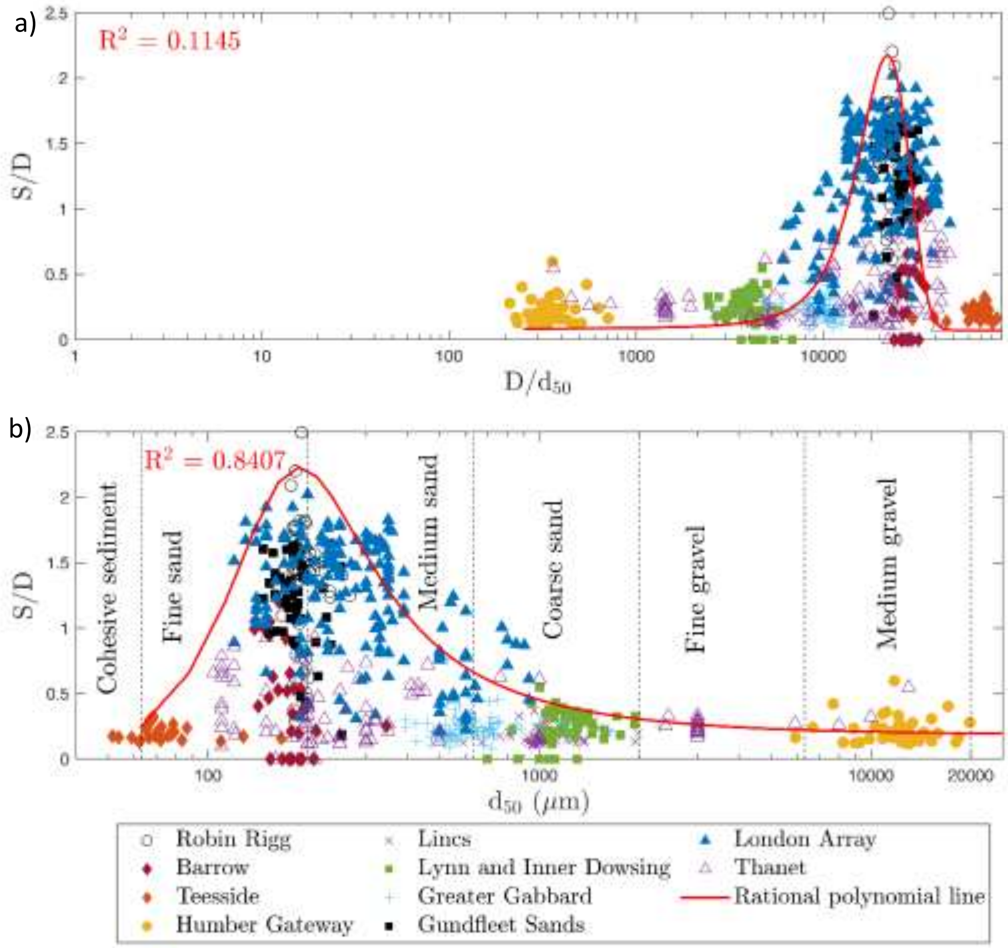


*Figure 8: Relative scour depths against (a) the relative grain size, and (b) grain size. The red rational polynomial line gives the approximate upper limit of S/D, based on the course of the 99th percentile, for various $\boldsymbol{d_{50}}$. Data points for London Array and Thanet OWFs are included from Melling (2015).*

*Figure 8a summarizes the findings from the PCA analysis (Figure 4) by plotting the relationship between the relative scour depth and relative grain size   across all the sampled locations. Figure 8b is also shown here to support figure 8a by representing the data in terms of the grain size, allowing the comparison of dimensional and non-dimensional $d_{50}$. Figure 8a, reveals no clear trend between relative scour depth and relative grain size, indicating that the dimensionless grain size ratio alone does not adequately capture the relationship between sediment properties and scour depth in field data. Sheppard et al. (2004) observed a clear trend of S/D decreasing for $^{D}/_{d_{50}} > 50$ in laboratory experiments, which is not consistent with our results. However, field data show much weaker dependence due to natural variability in sediment structure and hydrodynamic forcing*

*On the other hand, Figure 8b illustrates a discernible trend where the largest relative scour depths $S/D$ occur predominantly in fine to medium sands ($R^2$= 0.8407), as indicated by the rational polynomial line* *which approximates the upper limit of relative scour depth for various grain size. The trend shown in Fig. 8b is well explained. In general, the mobility potential of the sediments decreases with increasing grain size, which leads to lower relative scour depths for coarser sediments. Very fine sediments, on the other hand, are subject to the influence of cohesion forces that reduce their erodibility, which also leads to lower relative scour depths. Therefore, fine and medium sandy sediments have the largest scour potential, which is reflected in the data of Fig. 8b. The different symbols represent the OWF, highlighting the geographic spread and variability within the dataset. However, it is important to note that most of the data points fall within the range of fine to medium sands, potentially skewing the interpretation.*

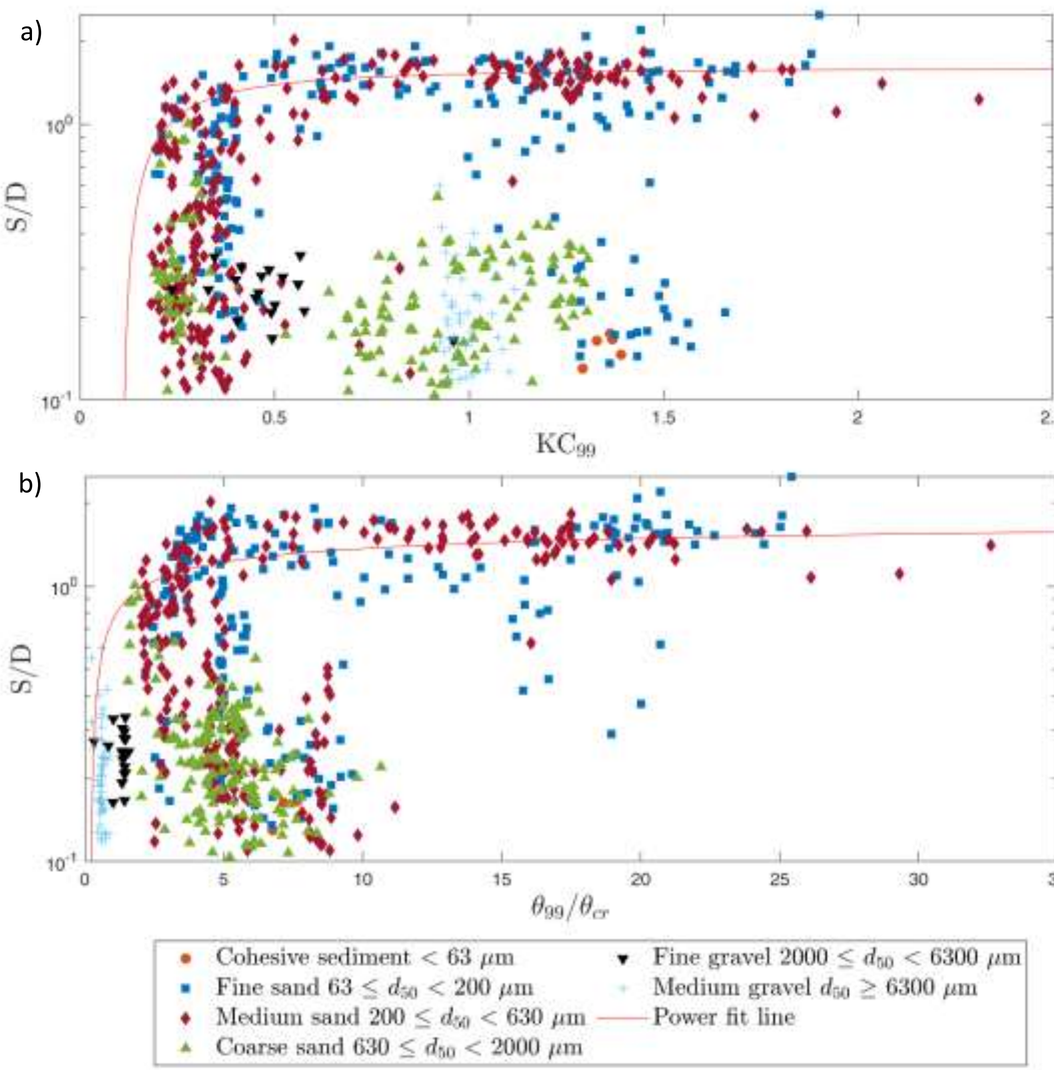


*Figure 9: a) Relative scour depth against the Keulegan-Carpenter number. b) Relative scour depth against the mobility parameter. Red line gives the power fit line based on the 99th quantile of the data of relative*

*scour depth for various $\boldsymbol{d_{50}}$. Data points for London Array and Thanet OWFs are included from Melling (2015).*

*The third and fourth parameters, that correlate with the relative scour depth, are the Keulegan-Carpenter number and the mobility parameter as identified by the PCA. Figure 9a shows the correlation between relative scour depth and $KC_{99}$, revealing a distinct increase of relative scour depth with increasing $KC_{99}$ up to $KC_{99} = 0.5$. Above this value, $S/D$ shows little variation with further increase of $KC_{99}$, which reaches a maximum value of 2.5 in this field dataset. Those results are generally consistent with findings from previous studies (e.g., Qu et al., 2024; Sumer & Fredsøe, 2002), which indicate that scour development is strongly dependent on $KC_{99}$ at lower values, but becomes less sensitive as $KC_{99}$ increases. However, experimental studies often focus on wave regimes with $KC$ numbers greater than 6, since it has been established that this is the threshold for generating a horseshoe vortex. Despite considering the 99th percentile of $KC$ numbers over the time period in question, the KC numbers are much smaller for the field conditions presented herein. This strengthens the argument for further scour research to focus on boundary conditions with low $KC$ values.*

*Figure 9b shows the correlation between relative scour depth and mobility parameter, comparing the Shields parameter with its critical threshold for sediment motion, and revealing a distinct increase of relative scour depth with increasing mobility parameter up to approximately $\theta_{99}/\theta_{cr}$ = 5. At higher mobility values (typically above 5–10), the increase in scour depth tends to stabilize. This trend aligns with experimental observations from Sumer et al. (2013), Chiew (1984), and others, which describe similar stabilization of scour depth under fully mobile conditions. Notably, the response also varies with sediment type: coarser sediments exhibit low $S/D$ values even at high mobility ratios, likely due to their higher resistance to entrainment and potential armoring effects. In contrast, finer sediments (e.g., $d_{50} < 200\ \mu m$) show a steeper increase in scour depth, reflecting their greater susceptibility to hydrodynamic conditions.*

*Overall, Figure 9a and 9b emphasize the nonlinear and sediment-dependent nature of scour formation. The separation of trends by soil class supports the need for sediment-specific scour prediction models, as also suggested in previous studies (e.g., Whitehouse et al., 2011; Sumer & Fredsøe, 2002). The results provide empirical evidence of this dependency using field-scale data, bridging a critical gap between controlled experiments and real-world conditions.*

2. Some other suggestions to improve the manuscript are listed as follows:

On Page 6, it is stated that the Froude number influences the scour depth. However, Fr is more related to the free-surface waves. How can it be related to the scour depth at the seabed? The analysis of the mechanism, which is stated to be related to the pressure gradients at the pile, is not clear. How can the free-surface waves affect the pressure gradients around the pile? How are the pressure gradients associated with the scour process? The authors should describe these problems in more detail, at least by providing some reference studies.

2. We would like to apologize for the confusion. While free-surface waves will also have a transient effect on the pressure gradient, in our analysis, the Froude number ($Fr$) is defined in the context of tidal current-induced flows around the monopile and is calculated as follows (see Table 2, equation 2):

$$Fr = \frac{U}{\sqrt{gh}}$$

Where $U$ is the near-bed current velocity and $h$ is the local water depth.

Large $Fr$ induces intensified inertial forces that produce a strong adverse pressure gradient at the upstream site of the pile. This results in early boundary layer separation from the seabed. The separated shear layer rolls into a horseshoe vortex, and the vortex' core strength increases with $Fr$. This amplifies bed shear stress around the scour perimeter and accelerates sediment erosion (Hu, 2021).
Laboratory and numerical studies under transitional Reynolds regimes affirm this mechanism. Corvaro et al. (2015) found that increasing $Fr$ results in larger vortex diameters and higher (bed shear stress $-\tau_b$) concentrations, leading to deeper equilibrium scour depths.

In response, lines 194- 203 on page 7 were modified and references as well as the definition of the $Fr_{99}$ were added:

*"The Froude number ($Fr_{99}$) and pile Reynolds number ($Re_{99}$) are used to characterize the flow conditions around the pile and their calculations are shown in Table 2, equations 2 and 3. The Froude number indicates whether the flow is dominated by gravitational or inertial forces. With increasing Froude number, stronger inertial forces produce a more pronounced adverse pressure gradient at the upstream face of the monopile. This promotes early boundary layer separation and enhances the strength of the horseshoe vortex system near the seabed, which increases local bed shear stress and accelerates sediment erosion. As shown by Hu (2021), these dynamics are key in amplifying scour. Similarly, Corvaro et al. (2015) found that higher Froude numbers lead to larger vortex structures and increased bed shear stress, resulting in deeper equilibrium scour depth. On the other hand, the Reynolds numbers provide information on whether the flow is laminar or turbulent and determine the characteristics of the vortex system around the pile."*

3. As an important component of the analysis, the process of performing the PCA should be elaborated in more detail. For example, how to arrange the current measurement data into matrices and how to compute the correlation angle should be introduced.

3. We thank the reviewer for this valuable comment. We have provided a better explanation in the methodology section 2.3, where it is explained how the current measurement data was arranged

into matrices and, how other studies used the PCA for scour data. See lines 296 – 319 on page 14-15:

*"In this study, the PCA was applied to a dataset of 692 OWES, including 460 from our analysis and an additional 232 OWES from London Array and Thanet OWF, based on Melling's (2015) data. The PCA was then performed using eight independent variables that contributed to the principal components. Those dimensionless variables were the relative water depth ($h/D$), Keulegan-Carpenter number ($KC_{99}$), mobility parameter ($\theta_{99}/\theta_{cr}$), Reynolds number ($Re$), Froude number ($Fr$), relative sediment size ($D/d_{50}$), flow intensity ($(\frac{U}{U_{cr}})_{99}$), and the relative scour depth ($S/D$). Following this, the data was organized into a matrix, with each row representing a specific OWES and each column representing a selected dimensionless variable. All the variables were extracted as representative values specific to the OWES, with the focus on the 99th percentile to capture extreme hydrodynamic conditions. Scour processes are more likely to occur in these extreme conditions because maximum scour depths usually develop during storm-induced events, rather than under mean or median values. Subsequently, the variables were standarized to ensure the comparability of the results..*

*In some studies, the PCA is used for reducing the number of dimensions (Harasti, 2022), or to help develop predictive models grouped by soil classes (Annad, 2023). However, the aim of this study was to keep all the principal components. This approach enabled the full exploration of the interdependence between physical drivers and scour response across sites. To interpret the relationships among the variables, a principal component analysis biplot was generated (Gabriel et al., 1971). In the biplot, variables are represented as vectors, and the angle between vectors indicates the degree of correlation. The strength of the correlation was quantified using the cosine of the angle (Jolliffe & Cadima, 2016), enabling us to assess the strength of association between each variable and scour variability ($S/D$) across different OWFs sites. Similar to previous studies that applied PCA for parameter selection in bridge pier or scour formula development (Harasti, 2022; Annad, 2023), this multivariate analysis provides a clearer understanding of which parameters dominate the scour process under real offshore conditions"*

4. On Page 17, the discussion on the influence of the water depth on the scour depth is not sufficient, especially regarding the unexpected decrease in the scour depth with the increasing water depth. The authors stated that it is expected that a large water depth led to a large boundary layer thickness. However, the boundary layer thickness is not necessarily related to the water depth and more associated with Re and seabed roughness. Furthermore, the discussion on the pressure fields is rather superficial. Why does the increasing water depth result in more uniform pressure fields? Why does thinner boundary layer lead to a large shear stress?

4. We thank the reviewer for this valuable comment. We have provided a response where, the unexpected decrease of the relative scour depth (S/D) with the increasing relative water depth (S/D) is explained, additional references were added. In response lines 455 – 476 (page 22) were modified:

*"In contrast, relative water depth has a strong negative correlation with relative scour depth in fine sand (Figure 5b) and medium sand (Figure 5c). This indicates that as relative water depth increases, relative scour depth tends to decrease in these finer soil classes. From a physical view, Melling (2015) found out that in similar substrates, relative scour depths agree well between different geographic locations and showed that turbines located in sandy sediments exhibit a strong influence of relative water depth on scour, suggesting geotechnical factors are less influential in coarser sediments. Although the observation that relative scour depth decreases as relative water depth increases might initially seem counterintuitive. This behavior is best explained through the transition between shallow-water and deep-water flow regimes. As flow approaches a pile, stagnation pressure develops on its upstream face, causing the flow to separate into an up-flow and a down-flow component. The down-flow is directed toward the bed and promotes the formation of a horseshoe vortex. Flow separation occurs at the stagnation point, defined as the location of maximum energy from the approaching flow at the pile face. The energy of the approach flow consists of hydrostatic and kinetic components, whose vertical distribution is governed by the boundary layer. In shallow water, the kinetic component dominates over hydrostatic pressure, resulting in a stagnation point located higher up the pile, near the water surface. This enhances down-flow and vortex activity, intensifying scour processes (Melville, 2008). Additionally, shallower water often features thinner boundary layers with higher velocity gradients near the seabed, potentially leading to greater bed shear stresses and increased sediment mobility. In contrast, in deeper water, hydrostatic pressure becomes more influential, leading to a more uniform pressure field across the pile face and shifting the stagnation point closer to the bed. This results in weaker down-flow and reduced vortex strength, thereby diminishing the scour depth (FHWA, 2012; Harris & Whitehouse, 2014). Furthermore, Link and Zanke (2004) observed that maximum relative scour depths tend to develop more slowly and reach lower values in deeper water depths, even under constant average flow velocity, due to reduced shear velocity over the undisturbed bed. This highlights that the relationship between relative water depth and scour is not necessarily linear.*

It is difficult to understand the influence of Fr on scour depth. Especially, as shown in Figure 6 (e), it seems that there are only two exceptional points, and the correlation is not strong.

We acknowledge the reviewer's concern about the apparently weak correlation between the Froude number ($Fr$) and scour depth, as shown in Figure 6(e). The limited number of data points exhibiting extreme $Fr$ values in our extensive dataset makes it difficult to discern a strong statistical relationship through PCA.

In this regard, lines 561– 565 (page 25), where the correlation between Fr and scour depth in fine gravel is described, were modified:

*"For fine gravel (Figure 6e), the PCA suggests a correlation between relative scour depth and the Froude number, but this is difficult to confirm visually due to the small sample size and narrow Froude number range. Since relative scour depth is comparatively small in this class, relationships are less clear, and parameters like Froude number come to the foreground that were not as prominent in finer sediments. A broader distribution of Froude number values would be necessary to confirm this more conclusively"*

4. On Page 30 from Line 592 to 597, it is stated that the wave dynamics play an important role in determining the scour depth. The authors should provide a more detailed discussion on this subject by estimating the KC number based on the wave height and water depth.

We acknowledge the request of the reviewer for a more detailed discussion of the significant role of wave dynamics on scour depth. As highlighted on Page 30, there is a correlation between higher wave heights from the northeast and increased scour depths. This observation underscores the strong influence of wave energy on seabed modification.

To provide a more quantitative analysis, we incorporated the into our revised analysis *(see Table 2, eq. 9)*. Additionally, lines 849 – 851 on page 41 were modified:

*"Figure 12D shows that the highest wave heights are observed coming from the northeast, with values exceeding 3.0 m, and lower wave heights propagating from the southwest. This gradient in wave height suggests a correlation with increased relative scour depths in regions exposed to higher wave energy, suggesting a strong link between wave dynamics and seabed modification. However, estimated $KC_{99}$ numbers remained relatively low across most sites, indicating limited wave-induced orbital motion near the seabed. This suggests that wave action plays a secondary role in scour development compared to currents. Similarly, Figure 12E highlights a larger number of strong currents coming from the southeast. These higher velocities correspond to areas with more pronounced relative scour depths, highlighting the role of strong currents in influencing sediment transport and depositional patterns."*

References:

Annad, Mohamed, Nadjib Hemaidi Zourgui, Abdelouahab Lefkir, Abderrahmane Kibboua, and Oussama Annad. "Scour-dependent seismic fragility curves considering soil-structure interaction and fuzzy damage clustering: A case study of an Algerian RC Bridge with shallow foundations." Ocean Engineering 275 (2023): 114157.

Chiew, Yee Meng. "Local scour at bridge piers." Publication of: Auckland University, New Zealand (1984).

Roulund, A., J. Sutherland, D. Todd, and J. Sterner. "Parametric equations for Shields parameter and wave orbital velocity in combined current and irregular waves." (2016).

Corvaro, Sara, Alessandro Mancinelli, and Maurizio Brocchini. "FLOW DYNAMICS OF WAVES PROPAGATING OVER DIFFERENT PERMEABLE BEDS." Coastal Engineering Proceedings 35 (2016): 35-35.

Gabriel, Karl Ruben. "The biplot graphic display of matrices with application to principal component analysis." Biometrika 58, no. 3 (1971): 453-467.

Hu, Ruigeng, Xiuhai Wang, Hongjun Liu, and Yao Lu. "Experimental study of local scour around tripod foundation in combined collinear waves-current conditions." Journal of Marine Science and Engineering 9, no. 12 (2021): 1373.

Jolliffe, Ian T., and Jorge Cadima. "Principal component analysis: a review and recent developments." Philosophical transactions of the royal society A: Mathematical, Physical and Engineering Sciences 374, no. 2065 (2016): 20150202.

Link, Oscar, and Ulrich Zanke. "On the time-dependent scour-hole volume evolution at a circular pier in uniform coarse sand." In Proc. 2nd International Conference on Scour and Erosion (ICSE). 2004.

Qu, Lili, Hongwei An, Scott Draper, Phil Watson, Ming Zhao, John Harris, Richard Whitehouse, and Di Zhang. "A review of scour impacting monopiles for offshore wind." Ocean Engineering 301 (2024): 117385.

Roulund, A., J. Sutherland, D. Todd, and J. Sterner. "Parametric equations for Shields parameter and wave orbital velocity in combined current and irregular waves." (2016).

Smith, J. Dungan, and S. R. McLean. "Spatially averaged flow over a wavy surface." Journal of Geophysical research 82, no. 12 (1977): 1735-1746.

Sheppard, D. Max, Gang Zhao, and Budianto Ontowirjo. "Local scour near single piles in steady currents." In Water resources engineering, pp. 1809-1813. ASCE, 1995.

Sheppard, D. M., B. Ontowirjo, and G. Zhao. “Conditions of Maximum Local Scour.” In Proceedings of Stream Stability and Scour at Highway Bridges, Resources Engineering Conference 1991–1998, edited by E. V. Richardson and P. F. Lagasse. Reston, VA: ASCE, 1999

Sumer, B. Mutlu, Thor U. Petersen, Luca Locatelli, Jørgen Fredsøe, Rosaria E. Musumeci, and Enrico Foti. "Backfilling of a scour hole around a pile in waves and current." Journal of Waterway, Port, Coastal, and Ocean Engineering 139, no. 1 (2013): 9-23.

Soulsby, Richard L., and R. JS Whitehouse. "Threshold of sediment motion in coastal environments." In Pacific Coasts and Ports' 97: Proceedings of the 13th Australasian Coastal and Ocean Engineering Conference and the 6th Australasian Port and Harbour Conference; Volume 1, pp. 145-150. Christchurch, NZ: Centre for Advanced Engineering, University of Canterbury, 1997.

Whitehouse, R. J. S., Harris, J. M., Sutherland, J., and Rees, J.: The nature of scour development and scour protection at onshore wind farm foundations, Mar. Pollut. Bull., 62(1), 73–88, 2011.

Whitehouse, Richard JS, and John Harris. "Scour prediction offshore and soil erosion testing." (2014).

Federal Highway Administration (FHWA). Evaluating scour at bridges (HEC-18, Publication No. FHWA-HIF-12-003). U.S. Department of Transportation (2012).

Zanke, Ulrich CE, Tai-Wen Hsu, Aron Roland, Oscar Link, and Reda Diab. "Equilibrium scour depths around piles in noncohesive sediments under currents and waves." Coastal Engineering 58, no. 10 (2011): 986-991.